Molecular determinants of homo- and heteromeric interactions of Junctophilin-1 at triads in adult skeletal muscle fibers

Daniela Rossi[a], Angela Maria Scarcella[a], Enea Liguori[a], Stefania Lorenzini[a], Enrico Pierantozzi[a], Candice Kutchukian[b], Vincent Jacquemond[b,c], Mirko Messa[d,e], Pietro De Camilli[d,e,f], and Vincenzo Sorrentino[a,1]

[a]Department of Molecular and Developmental Medicine, Molecular Medicine Section, University of Siena, 53100 Siena, Italy; [b]Institut NeuroMyoGène, Université Claude Bernard Lyon 1, F69622 Villeurbanne, France; [c]CNRS UMR 5310, INSERM U1217, F69622 Villeurbanne, France; [d]Department of Neuroscience, Kavli Institute for Neuroscience, Yale University School of Medicine, New Haven, CT 06510; [e]Department of Cell Biology, Kavli Institute for Neuroscience, Yale University School of Medicine, New Haven, CT 06510; and [f]HHMI, Yale University School of Medicine, New Haven, CT 06510

Edited by Clara Franzini-Armstrong, University of Pennsylvania School of Medicine, Philadelphia, PA, and approved June 24, 2019 (received for review December 18, 2018)

In adult skeletal muscles, 2 junctophilin isoforms (JPH1 and JPH2) tether the sarcoplasmic reticulum (SR) to transverse tubule (T-tubule) membranes, generating stable membrane contact sites known as triads. JPHs are anchored to the membrane of the SR by a C-terminal transmembrane domain (TMD) and bind the T-tubule membrane through their cytosolic N-terminal region, which contains 8 lipid-binding (MORN) motifs. By combining expression of GFP-JPH1 deletion mutants in skeletal muscle fibers with in vitro biochemical experiments, we investigated the molecular determinants of JPH1 recruitment at triads in adult skeletal muscle fibers. We found that MORN motifs bind $PI(4,5)P_2$ in the sarcolemma, but do not mediate the selective localization of JPH1 at the T-tubule compartment of triads. On the contrary, fusion proteins containing only the TMD of JPH1 were able to localize at the junctional SR compartment of the triad. Bimolecular fluorescence complementation experiments indicated that the TMD of JPH1 can form dimers, suggesting that the observed localization at triads may result from dimerization with the TMDs of resident JPH1. A second domain, capable of mediating homo- and heterodimeric interactions between JPH1 and JPH2 was identified in the cytosolic region. FRAP experiments revealed that removal of either one of these 2 domains in JPH1 decreases the association of the resulting mutant proteins with triads. Altogether, these results suggest that the ability to establish homo- and heterodimeric interactions with resident JPHs may support the recruitment and stability of newly synthesized JPHs at triads in adult skeletal muscle fibers.

T-tubule | excitation–contraction coupling | membrane contact sites

The endoplasmic reticulum (ER) has a multiplicity of functions, including regulation of Ca^{2+} homeostasis and lipid synthesis. To perform many of these functions, the ER contains a number of tethering proteins that mediate the establishment of specific membrane contact sites (MCSs) with other organelles (1, 2). In muscle cells, the complex organization of the sarcoplasmic reticulum (SR), together with the occurrence of peculiar MCSs between the SR and the plasma membrane (PM) of muscle fibers, from here on referred to as sarcolemma, represent key elements for regulating Ca^{2+} homeostasis and muscle contraction (3). In skeletal muscle, the SR is organized in longitudinal tubules (l-SR) that surround, like a sleeve, each myofibril. The close positioning of the l-SR around the myofibrils is mediated by an interaction between sAnk1.5, a transmembrane protein of the SR, and obscurin, a sarcomeric protein localized at the periphery of the myofibrils (4–7). At regular intervals, l-SR tubules converge into the so-called terminal cisternae, which represent the junctional SR (j-SR), since they participate in the formation of specialized muscle-specific MCSs with the surface sarcolemma or with the transverse tubules (T-tubules). T-tubules are infoldings of the sarcolemma that radially penetrate muscle cells (3). MCSs between the j-SR and the surface sarcolemma are called peripheral couplings, while MCSs with T-tubules are called dyads or triads depending on whether the T-tubule makes contact with 1 or 2 regions of the j-SR. In skeletal muscle, peripheral couplings and dyads are present in the early stages of differentiating myotubes, while both structures are gradually replaced by triads positioned at the borders between the A and I bands of the sarcomere in mature skeletal muscle fibers (3, 8, 9). The function of these muscle-specific MCSs is to support the structural organization of components of the excitation–contraction (e-c) coupling machinery that transduces depolarization of the sarcolemma into activation of Ca^{2+} release from the SR (10, 11). More precisely, the e-c coupling mechanism requires an interaction between the L-type voltage-gated Ca^{2+} channels on the sarcolemma (dihydropyridine receptors, DHPRs) and the Ca^{2+} channels on the SR (ryanodine receptors, RyRs). The latter, once activated, allow the release of the large amount of Ca^{2+} required to stimulate the actomyosin system and to generate force (12, 13). The tethering proteins responsible for the assembly of peripheral couplings, dyads and triads in skeletal muscle are Junctophilin-1 and Junctophilin-2 (JPH1 and JPH2), while only JPH2 is expressed in cardiac muscle (14). Studies based on gene knockout (KO) in

Significance

Triads are specialized stable membrane contact sites present in skeletal muscles fibers, where 2 junctophilin isoforms (JPH1 and JPH2) tether the sarcoplasmic reticulum to the transverse tubules (T-tubules), which are infoldings of the sarcolemma. Several muscle-specific proteins are localized at triads, where they participate in the excitation–contraction (e-c) coupling process, which consists of a series of functional events resulting in muscle fibers' contraction in response to electrical stimulation. Many reports have shown that JPH1, in addition to mediating the assembly of triads, can also interact with several proteins of the e-c coupling machinery. We report here that JPH1 and JPH2 can form homo- and heterodimers and that the transmembrane domain promotes the localization of JPH1, likely via interactions with endogenous JPHs.

Author contributions: D.R., P.D.C., and V.S. designed research; D.R., A.M.S., E.L., S.L., E.P., C.K., and M.M. performed research; D.R., V.J., and V.S. analyzed data; and D.R., V.J., P.D.C., and V.S. wrote the paper.

The authors declare no conflict of interest.

This article is a PNAS Direct Submission.

[1]To whom correspondence may be addressed. Email: vincenzo.sorrentino@unisi.it.

This article contains supporting information online at www.pnas.org/lookup/suppl/doi:10.1073/pnas.1820980116/-/DCSupplemental.

Published online July 17, 2019.

mice have shown that deletion of *Jph1* interfered with triad formation, while deletion of *Jph2* resulted in embryonic lethality due to altered heart development (14, 15). Two additional JPH genes (JPH3 and JPH4) are expressed in neurons, where they are involved in the formation of MCSs between the ER and the PM, which favor the interaction between RyRs and NMDA receptors and K^+ channels (16–20). More recently, JPH3 and JPH4 have also been shown to organize MCSs in pancreatic β-cells (21) and in T lymphocytes (22), respectively. All 4 JPH proteins share a common structural organization, with 8 conserved structural Membrane Occupation and Recognition Nexus (MORN) motifs at the N terminus. The first 6 MORN motifs are separated by the last 2 by a region of about 120 amino acids, referred to as the "joining region" (14, 23). MORN motifs were shown to mediate binding to the plasma membrane through interaction with membrane phospholipids (14, 24). The region containing the MORN motifs is followed by a putative α-helical region, by a "divergent linker region" with no homology between JPH subtypes, and by a transmembrane domain (TMD) at the C terminus, which anchors JPHs to the ER/SR membrane (14, 23). The average distance of 10 to 12 nm between T-tubule and SR membranes in a triad is compatible with JPHs acting as molecular bridges filling the gap between the 2 opposite membrane structures (3, 8, 14).

In addition to allowing the assembly of MCSs between the j-SR and the sarcolemma, JPHs also appear to engage in interactions with several proteins of the e-c coupling machinery, including DHPRs on the T-tubule, and RyRs, triadin, and calsequestrin on the SR (25–29). Interactions between JPH1, JPH2, and these proteins may contribute to the assembly of e-c coupling components at triads. Interestingly, decreased levels and/or mutations in JPHs have been observed in patients with cardiac diseases (30–35). In particular, JPH2 mislocalization and T-tubule remodeling are frequently associated with heart failure, suggesting that JPHs are required in the assembly, but also in the maintenance of the dyad geometry and function in mature cardiac cells (26, 36–40).

Here we analyzed the role of different regions of JPH1 with respect to the recruitment and stable association with triads in adult skeletal muscle fibers. We report that the MORN motifs mediate binding to the sarcolemma via an interaction with $PI(4,5)P_2$, a phosphoinositide concentrated in this membrane (41). However, this interaction occurs along the entire sarcolemma and not only at T-tubules. In contrast, we found that a GFP fusion protein containing the TMD of JPH1 selectively localized at the junctional domain of the SR, likely because of its ability to form homodimers. Immunoprecipitation and pull-down experiments revealed that JPH1 and JPH2 contain a second site of interaction in the cytosolic regions. Altogether, these results suggest that recruitment of newly synthesized JPHs at triads in adult skeletal muscle fibers may result from the establishment of interactions with endogenous JPHs.

Results

JPH1 and JPH2 Bind to $PI(4,5)P_2$ and Organize ER-PM Contact Sites in HeLa Cells Comparable to Those Assembled by E-Syt3. Following transfection in HeLa cells, a fusion protein containing the ER resident protein, Sec61β, tagged with mCherry (mCherry-Sec61β), was homogeneously distributed throughout the ER. No obvious enrichment was observed in the cortical ER, i.e., the ER portion juxtaposed to the PM, labeled with the GFP-tagged Pleckstrin Homology (PH) domain of the Phospholipase Cδ1 (PLC) (GFP-PH-PLCδ1, Fig. 1 *A–C*). When coexpressed with plasmids encoding either GFP-JPH1, GFP-JPH2, or GFP-E-Syt3, a ubiquitously expressed protein that promotes the formation of cortical ER in eukaryotic cells (42), a pool of the mCherry-Sec61β signal was shifted to the cortical region of the cells, where it colocalized with these GFP-tagged proteins as a consequence of the assembly of MCSs induced by each of these proteins (Fig. 1 *D–F*, *G–I*, and *J–L*, respectively). In addition, when GFP-JPH1 and mCherry-E-Syt3 were coexpressed in HeLa cells, they showed an overlapping pattern of localization, mainly at the cortical region of the cell (Fig. 1 *M–O*). Altogether, these results indicate that, when expressed in nonexcitable cells, JPH1, JPH2, and E-Syt3 support the assembly of comparable MCSs, in agreement with previously reported results (14, 42, 43).

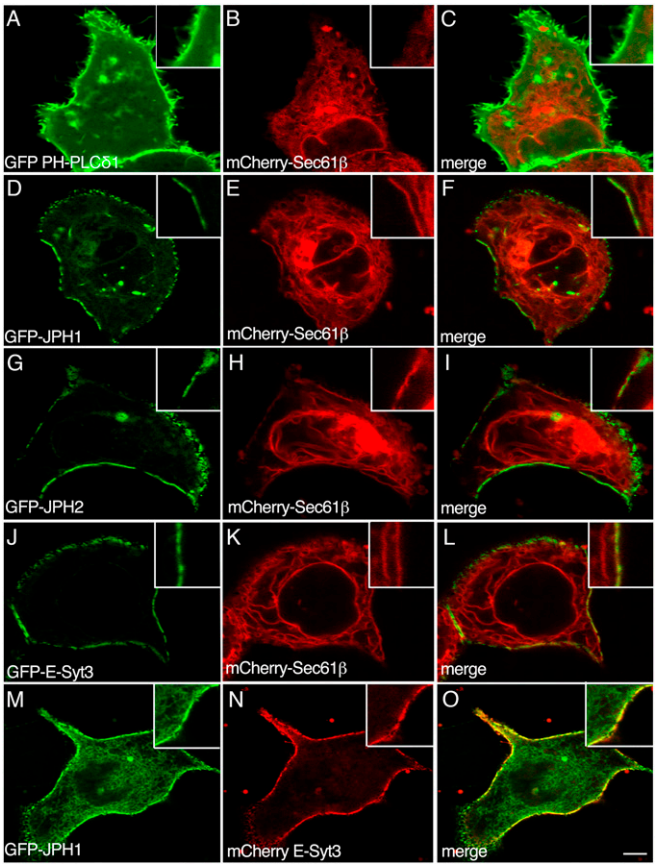

Fig. 1. Assembly of ER-PM contact sites in HeLa cells expressing recombinant GFP-JPHs or GFP-E-Syt3. Live imaging of HeLa cells transfected with plasmids encoding the GFP-tagged PH domain of the PLC (GFP-PH-PLCδ1) (*A*), Junctophilin-1 (GFP-JPH1) (*D* and *M*), Junctophilin-2 (GFP-JPH2) (*G*), Extended Synaptotagmin-3 (GFP-E-Syt3) (*J*), or mCherry-tagged E-Syt3 (mCherry E-Syt3) (*N*), and Sec61β (mCherry-Sec61β) (*B*, *E*, *H*, and *K*). *C*, *F*, *I*, *L*, and *O* are merged images. *Insets* show higher magnification of selected regions of the PM of transfected cells. Scale bar, 5 μm.

The interaction of E-Syts with the PM is mediated by the binding to $PI(4,5)P_2$ through the C2 domains present in the C-terminal region (42). It is known that MORN motifs interact with phospholipids in the PM (14, 24). We thus tested the effect of $PI(4,5)P_2$ depletion on GFP-JPH1 localization in HeLa cells. To this aim, we overexpressed a recombinant muscarinic acetylcholine receptor to achieve extensive activation of the endogenous PLC (42). In untreated cells, the iRFP-PH-PLCδ1 protein, used as a $PI(4,5)P_2$ probe, was localized at the PM (*SI Appendix*, Fig. S1 *D–F*). Depletion of membrane $PI(4,5)P_2$, following activation of PLC with 10 μM Oxo-M, resulted in dispersion of the iRFP fluorescence to the interior of the cell. Addition of 50 μM atropine to block PLC activation allowed the recovery of iRFP-PH-PLCδ1 localization at the PM (Movie S1). Similarly, following addition of Oxo-M to HeLa cells expressing GFP-JPH1, most of the fluorescence signal redistributed from the PM to the cytoplasmic ER domain. Addition of atropine restored localization of GFP-JPH1 at the PM (*SI Appendix*, Fig. S1 *A–C* and

PHYSIOLOGY

Movie S2). Altogether, these results suggest that the interaction of GFP-JPH1 with the PM requires PI(4,5)P_2. Similar results were also observed with GFP-JPH2 (Movie S3).

JPH1 and JPH2, but Not E-Syt3, Are Selectively Enriched at Triads in Skeletal Muscle Fibers. Unlike HeLa cells, the sarcolemma of mature skeletal muscle fibers forms specialized domains, the T-tubules, which are tethered by JPHs to specialized domains of the SR, the j-SR, to form the triads. The localization of GFP-JPH1, JPH2, and E-Syt3 was analyzed in adult mouse flexor digitorum brevis (FDB) muscle fibers following in vivo electroporation. As expected, GFP-JPH1 and GFP-JPH2 selectively localized at triads (Fig. 2 *A–F* and Fig. 2 *G–I*, respectively), identified with antibodies against endogenous RyR and appearing as a double row of fluorescent dots flanking the Z-disk, decorated with antibodies against α-actinin. The pattern observed with GFP-JPH1 and GFP-JPH2 is indistinguishable from that obtained by staining fibers with antibodies against RyR and triadin or against RyR and DHPR (*SI Appendix*, Fig. S2 *A–F*). No fluorescence signal specific for GFP-JPH1 or GFP-JPH2 was detected at the fiber periphery on the surface sarcolemma (Fig. 2 *A–F* and Fig. 2 *G–I*, respectively). On the contrary, the fluorescence signal of GFP-E-Syt3 was detected both at triads and at the surface sarcolemma (Fig. 2 *J–L*). Given that T-tubules are continuous with the surface sarcolemma, and j-SR with the membrane of the l-SR, the selective localization of newly synthesized GFP-JPHs at triads in FDB muscle fibers must result from a specific "targeting mechanism."

MORN Motifs Do Not Confer Selectivity for the T-Tubule Membrane. To investigate the domain(s) of JPH1 that mediates its selective association to triads, a series of plasmids encoding GFP-JPH1 deletion mutants was generated and expressed in FDB muscle fibers (*SI Appendix*, Fig. S3*A*). At variance with the full-length GFP-JPH1 protein that is excluded from the surface sarcolemma, the GFP-JPH1 fusion protein lacking the TMD, but containing all 8 MORN motifs and the cytosolic region (GFP-JPH1ΔTMD), was detected at the entire sarcolemma, i.e., T-tubules and surface sarcolemma (Fig. 3 *A–C*). This localization pattern differs from the one obtained following staining with antibodies against the endogenous RyR, which is strictly confined at triads and not found at the surface sarcolemma (*SI Appendix*, Fig. S2 *G–I*), and resembles the one observed with the PI(4,5)P_2 probe GFP-PH-PLCδ1 and GFP-E-Syt3 that localize at the entire sarcolemma and are not restricted at triads (*SI Appendix*, Fig. S4 *C* and *D*).

To also verify whether in skeletal muscle the interaction of JPH1 with the sarcolemma requires PI(4,5)P_2, we performed experiments of PI(4,5)P_2 depletion in skeletal muscle fibers coexpressing a mRFP-tagged JPH1ΔTMD protein and the voltage-sensing phosphoinositide phosphatase (VSP). VSP is a nonchannel protein which can be activated by strong membrane depolarization, resulting in rapid depletion of PI(4,5)P_2 at the sarcolemma by selective removal of the phosphate at the 5-position without concomitant increase in DAG and Ca^{2+}, as happens with PLC activation (44, 45). VSP activation by whole cell voltage clamp resulted in decrease of the fluorescence signal in the triadic region, accompanied by a parallel increase of the fluorescence signal outside the triad, consistent with partial translocation of the mRFP-JPH1ΔTMD protein from the triad to the cytosol (*SI Appendix*, Fig. S5). These results, in agreement with the data obtained in HeLa cells, indicate that, also in skeletal muscle fibers, binding of MORN motifs to the sarcolemma requires PI(4,5)P_2. Indeed, similarly to GFP-JPH1ΔTMD, also GFP-E-Syt3 and GFP-PH-PLCδ1 proteins, which bind PI(4,5)P_2 through C2 and PH domains, respectively, are equally distributed between the surface sarcolemma and T-tubules (*SI Appendix*, Fig. S4). Accordingly, binding to PI(4,5)P_2 is likely not to represent the determinant for the selective targeting of newly synthesized GFP-JPHs to triads.

The TMD of JPH1 Localizes at the Junctional Compartment of the SR. Additional GFP-JPH1 deletion mutants were prepared (*SI Appendix*, Fig. S3*A*) and their localization in skeletal muscle fibers analyzed. GFP-JPH1 mutants lacking the first 6 MORN motifs (GFP-JPH1ΔMORN I-VI) or all 8 MORN motifs (GFP-JPH1ΔMORN I-VIII) were both localized at triads in FDB muscle fibers (Fig. 3 *D–I*). This indicates that partial or even complete deletion of MORN motifs does not affect the selective localization at triads and suggests that this is likely dependent on signals provided by regions of the protein other than MORN. Expression of a GFP-JPH1 mutant lacking the MORN motifs and most of the cytoplasmic region (GFP-JPH1Δ1–537) still resulted in localization of this mutant at triads, and, in particular, at the j-SR compartment of the triad (Fig. 3 *J–L*). Finally, a GFP fusion protein (GFP-TMD-JPH1) containing only the last C-terminal 26 amino acids, which correspond to the TMD of JPH1, was expressed in FDB muscle fibers. Surprisingly, this mutant protein also showed a typical triadic localization (Fig. 3 *M–O*), indicating that the TMD of JPH1 is selectively retained at the junctional compartment of the SR, regardless of the presence of any other protein domains.

To further support this point, we investigated whether the TMD of JPH1 could drive the localization of a protein of the l-SR to the j-SR. We thus generated expression plasmids coding for a GFP-tagged Sec61β protein, a protein of the l-SR, and for a GFP-Sec61β mutant where the TMD of Sec61β was replaced by the TMD of JPH1 (GFP-Sec61β/TMD-JPH1). When expressed in FDB muscle fibers, GFP-Sec61β yielded a fluorescence signal localized in correspondence with the Z-disk (Fig. 4 *A*, *a–c*), as expected for a protein of the l-SR (46, 47). In contrast, GFP-Sec61β/TMD-JPH1 showed a selective triadic signal, further confirming the ability of the TMD of JPH1 to localize at the j-SR compartment of the triad (Fig. 4 *A*, *d–f*).

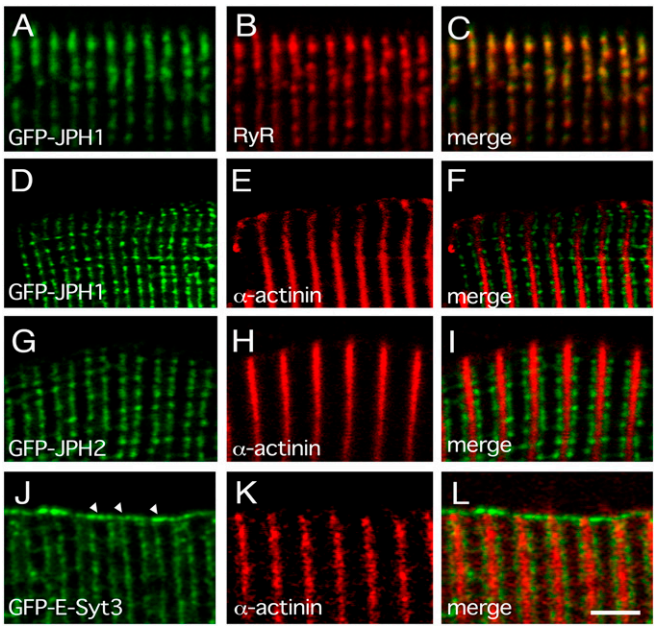

Fig. 2. Expression of recombinant GFP-JPHs or GFP-E-Syt3 in adult mouse FDB muscle fibers. Confocal images of adult mouse FDB muscle fibers expressing plasmids encoding GFP-JPH1 (*A* and *D*), GFP-JPH2 (*G*), or GFP-E-Syt3 (*J*). Fibers were counterstained with primary polyclonal antibodies against RyR (*B*) or monoclonal antibodies against α-actinin (*E*, *H*, and *K*), both revealed with Cy3-conjugated secondary antibodies. *C*, *F*, *I*, and *L* are merged images. Arrowheads indicate the surface sarcolemma. Scale bar, 2.5 μm.

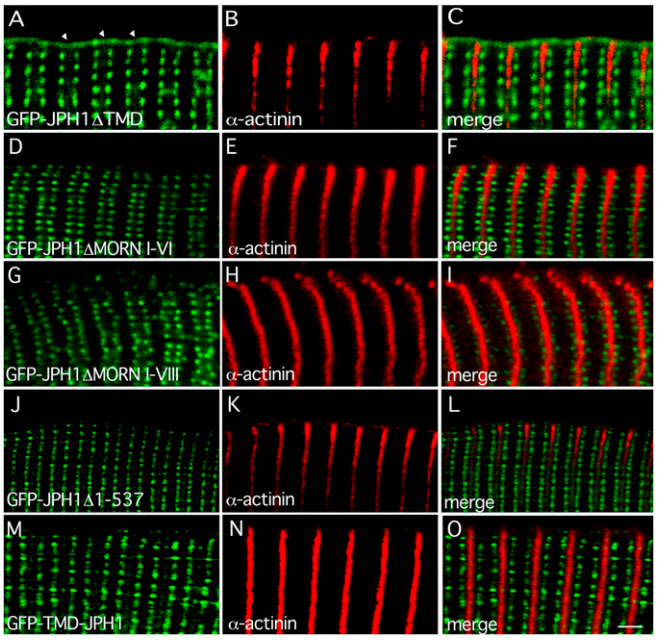

Fig. 3. Expression of GFP-JPH1 deletion mutants in adult mouse FDB muscle fibers. Confocal images of adult mouse FDB muscle fibers expressing plasmids encoding GFP-tagged Junctophilin-1 deleted of the TMD (GFP-JPH1ΔTMD) (*A*), the MORN I-VI (GFP-JPH1ΔMORN I-VI) (*D*), the MORN I-VIII (GFP-JPH1ΔMORN I-VIII) (*G*), or the amino acid region 1 to 537 (GFP-JPH1Δ1–537) (*J*), and GFP-tagged TMD of JPH1 (GFP-TMD-JPH1) (*M*). Fibers were counterstained with primary monoclonal antibodies against α-actinin and revealed with Cy3-conjugated anti-mouse secondary antibodies (*B*, *E*, *H*, *K*, and *N*). *C*, *F*, *I*, *L*, and *O* are merged images. Arrowheads indicate the surface sarcolemma. Scale bar, 2.5 μm.

Two Amino Acid Residues in the TMD of Muscle-Specific JPHs Are Required for Protein Localization at the j-SR. We next verified the localization of GFP fusion proteins containing the TMDs of JPH2, JPH3, and JPH4 isoforms (GFP-TMD-JPH2, GFP-TMD-JPH3, and GFP-TMD-JPH4, respectively). Expression of these proteins in FDB muscle fibers showed that only GFP-TMD-JPH2, like GFP-TMD-JPH1, localized at the j-SR compartment of the triad (Fig. 4 *B*, *a–f*), while the fluorescence signal of GFP-TMD-JPH3 and GFP-TMD-JPH4 did not yield a triadic signal, but was distributed in wide transversal lines, centered on the Z-disk, as expected for proteins of the l-SR (Fig. 4 *B*, *g–l*). Comparison of the amino acid sequences of JPH TMDs revealed a 77.27% identity between the TMD of JPH1 and that of JPH2, while the identity with the JPH3 or JPH4 TMDs was 59.09% and 40.91%, respectively (*SI Appendix*, Fig. S3*B*). In particular, the TMDs of JPH1 and JPH2 share 2 amino acids (Val^{656} and His^{657}), which are not present in the TMDs of JPH3 and JPH4, where they are replaced by Ile^{740} and Asn^{741} in the sequence of JPH3 and by Ser^{624} and Gln^{625} in the sequence of JPH4. To test the role of Val^{656} and His^{657} in conferring to the TMD of JPH1 and JPH2 the ability to selectively localize at the j-SR compartment of the triad, we replaced these amino acids with Ile and Asn from the TMD of JPH3 or with Ser and Gln from the TMD of JPH4. These substitutions resulted in loss of localization at the j-SR compartment of the triads of GFP-TMD-JPH1(VH > IN) and GFP-TMD-JPH1(VH > SQ) that, conversely, localized at the l-SR (Fig. 4 *C*, *a–f*). On the contrary, the replacement of amino acids Ile^{740} and Asn^{741} in the TMD of JPH3 with amino acids Val and His, resulted in the localization of the resulting fusion protein, GFP-TMD-JPH3(IN > VH), at the j-SR, with a distribution comparable to that observed with GFP-TMD-JPH1 (Fig. 4 *C*, *g–i*).

Bimolecular Fluorescence Complementation Assay (BiFC) Reveals That the TMD of JPH1 Can Form Dimers. The BiFC assay was used to verify whether localization of GFP-TMD-JPH1 at triads results

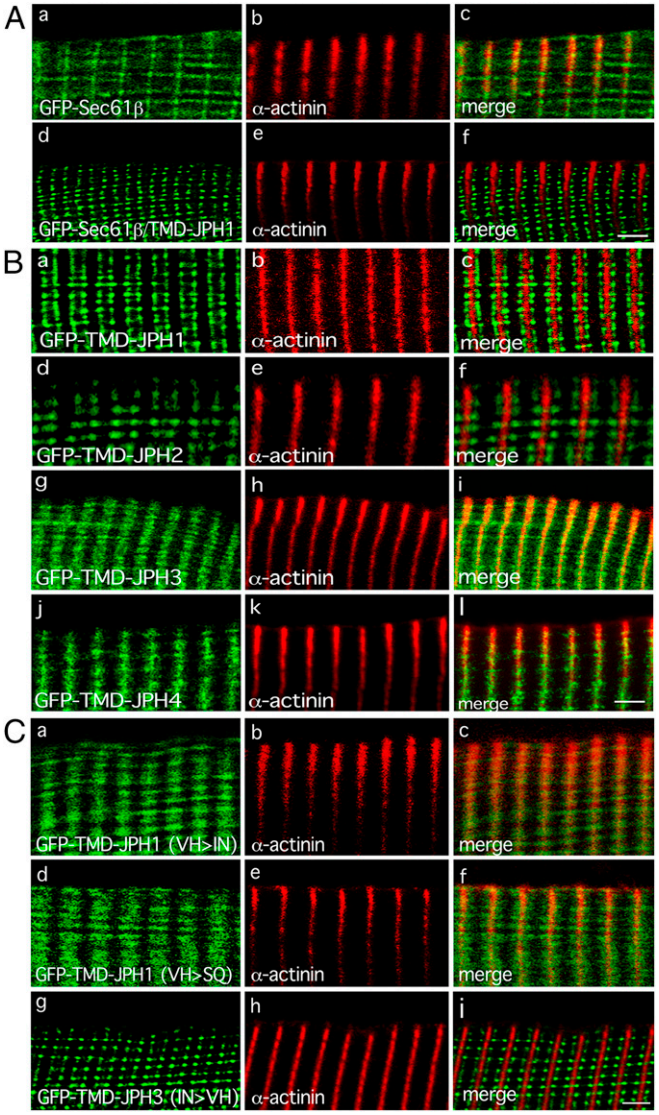

Fig. 4. Expression of GFP-TMDs of JPHs in adult mouse FDB muscle fibers. (*A*) Confocal images of adult mouse FDB muscle fibers electroporated with plasmids encoding GFP-tagged Sec61β (GFP-Sec61β) (*a*) or Sec61β in which the TMD sequence was replaced by that of JPH1 (GFP-Sec61β/TMD-JPH1) (*d*). *c* and *f* are merged images. Fibers were counterstained with primary monoclonal antibodies against α-actinin, revealed with Cy3-conjugated anti-mouse secondary antibodies (*b* and *e*). Scale bar, 3 μm. (*B*) Confocal images of adult mouse FDB muscle fibers electroporated with plasmids encoding GFP-tagged TMD of JPH1 (GFP-TMD-JPH1) (*a*), TMD of JPH2 (GFP-TMD-JPH2) (*d*), TMD of JPH3 (GFP-TMD-JPH3) (*g*), and TMD of JPH4 (GFP-TMD-JPH4) (*j*). *c*, *f*, *i*, and *l* are merged images. Fibers were counterstained with primary monoclonal antibodies α-actinin and Cy3-conjugated anti-mouse secondary antibodies (*b*, *e*, *h*, and *k*). Scale bar, 3 μm. (*C*) Confocal images of adult mouse FDB muscle fibers electroporated with plasmids encoding GFP-tagged TMD of JPH1 mutated in amino acids Val^{656} and His^{657} to Ile and Asn, respectively [GFP-TMD-JPH1(VH > IN)] (*a*), GFP-tagged TMD of JPH1 mutated in amino acids Val^{656} and His^{657} to Ser and Gln, respectively [GFP-TMD-JPH1(VH > SQ)] (*d*), GFP-tagged TMD of JPH3 mutated in amino acids Ile^{740} and Asn^{741} to Val and His, respectively [GFP-TMD-JPH3(IN > VH)] (*g*). *c*, *f*, and *i* are merged images. Fibers were counterstained with primary monoclonal antibodies against α-actinin, revealed with Cy3-conjugated anti-mouse secondary antibodies (*b*, *e*, and *h*). Scale bar, 2.5 μm.

PHYSIOLOGY

from homomeric interactions with resident JPH1 proteins. To this aim, two nonfluorescent fragments from the Venus protein (VN173: amino acids 1 to 173 and VC155: amino acids 155 to 238) were fused with the TMD of JPH1 to generate pBiFC-VN173-TMD-JPH1 and pBiFC-VC155-TMD-JPH1. As control, the TMD of JPH4, which does not localize at triads, was cloned into pBiFC vectors (pBiFC-VN173-TMD-JPH4 and pBiFC-VC155-TMD-JPH4). Confocal laser scan microscope analysis showed that BiFC signals were observed only when primary rat myotubes were cotransfected with pBiFC-VN173-TMD-JPH1 and pBiFC-VC155-TMD-JPH1 (Fig. 5 *A*, *a*). On the contrary, no specific fluorescence signal was observed when cells were cotransfected with pBiFC-VN173-TMD-JPH1 and pBiFC-VC155-TMD-JPH4, indicating that the recombinant TMDs of JPH1 can form homodimers, while they do not interact with the TMDs of JPH4 (Fig. 5 *A*, *b*). In addition, no BiFC signal was observed upon cotransfection of pBiFC-VN173-TMD-JPH4 and pBiFC-VC155-TMD-JPH4, indicating that the TMDs of JPH4 do not dimerize (Fig. 5 *A*, *c*). Parallel results were observed when the BiFC analysis was performed in HeLa cells, suggesting that dimerization of TMDs of JPH1 does not require a muscle-specific environment (Fig. 5 *A*, *d–f* and *SI Appendix*, Table S1).

The "Joining Region" of JPHs Represents an Additional Dimerization Site. We previously reported that GFP-JPH1 shows a reduced mobility when localized at triads in differentiated myotubes (46). The dynamic properties of full-length GFP-JPH1 and selected GFP-JPH1 deletion mutants were evaluated in 12-d differentiated myotubes by fluorescence recovery after photobleaching (FRAP) experiments (Fig. 5*B*). Cells expressing low levels of GFP fluorescence were selected to avoid potential problems due to overexpression. These experiments showed that, while the mobile fraction of the full-length GFP-JPH1 protein was 32.28 ± 12.56%, that of each of the JPH1 mutants analyzed (i.e., lacking all MORN motifs [GFP-JPH1ΔMORNI-VIII], deleted of the TMD [GFP-JPH1ΔTMD], and containing only the JPH1 TMD region [GFP-TMD-JPH1]) was significantly higher (59.67% ± 20.1, 74.28 ± 8.94%, and 84.5 ± 14.51, respectively). These results suggest that the observed lower mobility of the full-length JPH1 may result from the assembly of the MCSs and/or from additional interactions simultaneously occurring at different protein sites, other than the one mediated by the TMD. Indeed, the mobile fraction of GFP-JPH1 measured in nonmuscle cells was significantly higher than that measured in differentiated myotubes (46). This suggests that the dynamic properties of

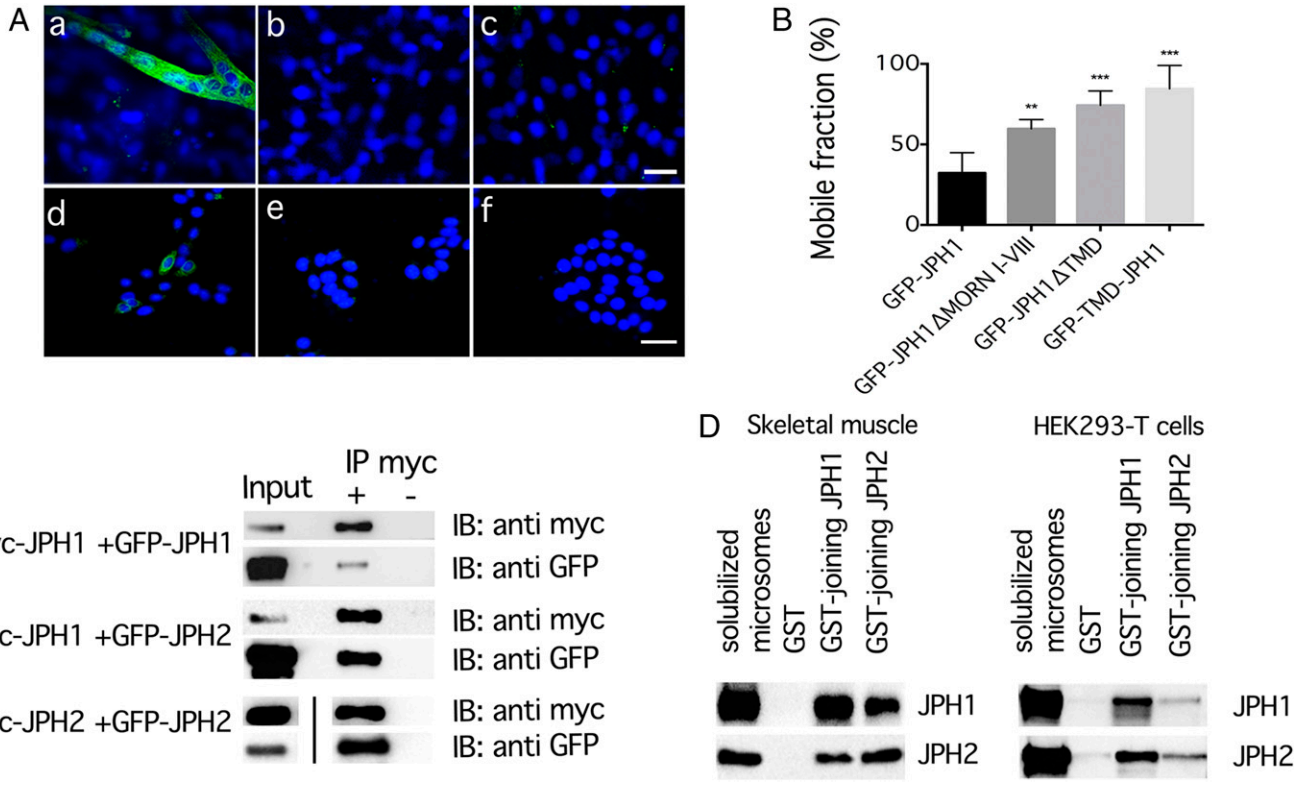

Fig. 5. (*A*) BiFC assay in 5-d differentiated rat primary myotubes and HeLa cells. BiFC assay was performed on 5-d differentiated myotubes (*a–c*) or HeLa cells (*d–f*) expressing either pBiFC-VN173-JPH1TMD and pBiFC-VC155-JPH1TMD (*a* and *d*) or pBiFC-VN173-JPH1TMD and pBiFC-VC155-JPH4TMD (*b* and *e*) or pBiFC-VN173-JPH4TMD and pBiFC-VC155-JPH4TMD (*c* and *f*). Scale bar, 15 μm. (*B*) FRAP analysis on 12-d differentiated rat primary myotubes expressing GFP-JPH1 and GFP-JPH1 deletion mutants. FRAP analysis was performed on 12-d differentiated myotubes expressing either GFP-JPH1 or GFP-JPH1 deletion mutants. Data are expressed as percentage of mobile fraction ± SEM; *n* values are as follows: GFP-JPH1 ($n = 20$); GFP-JPH1ΔMORN I-VIII ($n = 12$), GFP-JPH1ΔTMD ($n = 7$), and GFP-TMD-JPH1 ($n = 10$). Asterisks indicate statistical significance compared with the mobile fraction of GFP-JPH1, as evaluated by the Kruskal–Wallis multiple comparisons test (**$P \leq 0.05$; ***$P \leq 0.01$). (*C*) Immunoprecipitation experiments on HEK293T cells coexpressing myc-JPH1 and GFP-JPH1 or myc-JPH1 and GFP-JPH2, or myc-JPH2 and GFP-JPH2. Total lysates from HEK293T cells were immunoprecipitated with anti-myc conjugated agarose beads. Immunocomplexes were separated by SDS/PAGE, transferred to nitrocellulose membranes, and detected by mouse monoclonal anti-myc or anti-GFP antibodies. The vertical black line at *Bottom* indicates that an unrelated lane was eliminated from the figure. (*D*) GST pull-down experiments on the microsomal fraction of mouse skeletal muscles and of HEK293T cells. A total of 500 μg of the microsomal fraction from mouse skeletal muscles or HEK293T cells expressing either GFP-JPH1 or GFP-JPH2 was used in GST pull-down experiments using GST-joining JPH1 or GST-joining JPH2 fusion proteins. Proteins were separated by SDS/PAGE, transferred to nitrocellulose membranes, and detected by specific antibodies. A total of 30 μg of solubilized microsomes was loaded as control.

GFP-JPH1 at triads result from a combination of MCSs assembly and interactions with muscle-specific proteins.

Several laboratories have reported evidence indicating that JPH1 can establish interactions with other e-c coupling proteins, including RyR1, triadin, calsequestrin 1, and DHPR (25, 27–29). We thus wanted to verify whether JPH1 can also form homodimers or even heterodimers with JPH2. To this aim, HEK293T cells were cotransfected with plasmids encoding GFP-JPH1 and myc-JPH1, GFP-JPH2 and myc-JPH1, or GFP-JPH2 and myc-JPH2. As shown in Fig. 5*C*, coimmunoprecipitation experiments revealed that JPH1 and JPH2 can both form homodimers, but also heterodimers. Previous experiments had shown that a GST fusion protein containing the joining region was able to pull down the DHPR α_{1s} subunit (27). We then tested whether this region may also mediate homo- and heteromeric interactions between JPH1 and JPH2. In vitro pull-down experiments were performed with GST fusion proteins containing the joining region of JPH1 or JPH2 (GST-joining-JPH1 or GST-joining-JPH2) and solubilized microsomal proteins from mouse skeletal muscle tissue lysates. As shown in Fig. 5*D*, both GST-joining-JPH1 and GST-joining-JPH2 proteins were able to pull down JPH1 and JPH2 from muscle lysates, indicating that the joining region of the two proteins may mediate homo- and heterodimer formation. Pull-down experiments were also performed with GFP-JPH1 and GFP-JPH2 expressed in HEK293T cells. These experiments indicated that the GST-joining-JPH1 protein was able to pull down GFP-JPH1 and, to a lesser extent, GFP-JPH2. Similar results were observed in pull-down experiments with the GST-joining-JPH2 protein (Fig. 5*D*). Altogether these results indicate that homo- and heteromeric interactions between JPH1 and JPH2 result from direct protein-protein interactions.

Discussion

We report here results from experiments aimed at investigating the molecular determinants responsible for triad recruitment and association of JPH1 in adult skeletal muscle fibers.

Experiments performed in HeLa cells showed that GFP-JPH1 localizes at the cortical ER, where it mediates the formation of MCSs along the entire plasma membrane. This localization was similar to that observed with GFP-E-Syt3, a nonmuscle specific ER-PM tethering protein. However, when expressed in skeletal muscle fibers, GFP-JPH1 localized selectively at triads and was excluded from the surface sarcolemma and the longitudinal SR. In contrast, MCSs mediated by GFP-E-Syt3 did not show any specific selectivity for triads but were equally distributed along the entire sarcolemma. These results indicate that muscle-specific mechanisms restrict the localization of recombinant GFP-JPH1, but not that of GFP-E-Syt3, at triads.

Aiming to identify the domain(s) responsible for JPHs selective recruitment and localization at triads in adult skeletal muscle fibers, we generated a series of plasmids encoding GFP-JPH1 deletion mutants and expressed them in FDB muscle fibers. Interestingly, we found that a JPH1 mutant lacking the TMD (GFP-JPH1ΔTMD) localized at the entire sarcolemma, i.e., T-tubules and surface sarcolemma. This localization may be explained by the observed ability of MORN motifs to bind $PI(4,5)P_2$. Indeed, experiments with the $PI(4,5)P_2$ probe GFP-PH-PLCδ showed that this phospholipid appears to be equally distributed between T-tubules and the surface sarcolemma. Therefore, in the absence of the TMD, which anchors the protein to the j-SR compartment of triads, localization of the GFP-JPH1ΔTMD mutant mirrors the distribution of $PI(4,5)P_2$. Accordingly, these experiments indicate that MORN-mediated interactions with $PI(4,5)P_2$ is only 1 of the components of a coincidence detection mechanism that restricts JPH1 to triads.

On the other hand, we found that a GFP fusion protein containing the TMD of JPH1 localized only at the j-SR, yielding the typical double rows of fluorescent dots flanking the Z-disk. Interestingly, this property was observed only for the TMDs of the muscle-specific JPH1 and JPH2 isoforms. Two amino acids, Val^{656} and His^{657}, present in the TMDs of JPH1 and JPH2, but not in those of JPH3 and JPH4, appear to be critical for the localization at the j-SR. In fact, their substitution abolished the selective localization of the TMD of JPH1 at the j-SR, while introduction of these 2 amino acids in the TMD of JPH3 resulted in the localization of the resulting protein at the j-SR domain.

Results from BiFC assays indicated that the TMDs of JPH1 can form homodimers. This suggests that dimerization may promote the recruitment of the GFP-JPH1-TMD protein at the j-SR compartment of the triad, via interaction with resident JPH1, causing the exclusion of the full-length JPH1 from the surface sarcolemma. Although we have no evidence that the Val^{656} and His^{657} residues contribute specific structural determinant for JPH1 TMD dimerization, given that the corresponding residues in JPH4 TMD represent nonconservative changes, we hypothesize that lack of dimerization between JPH1 and JPH4 TMDs may result from differences in the physical and chemical properties of the amino acids at these positions that would limit the interaction between the surfaces of the 2 α-helices formed by these TMDs.

FRAP experiments indicated that the GFP-JPH1ΔMORN I-VIII and GFP-JPH1-TMD mutants, even if able to localize at triads, displayed an increased mobility compared with that observed with full-length JPH1. This increase in protein mobility could be explained by the absence, in these 2 mutants, of the "joining region" that we found to contribute to the assembly of JPH1 and JPH2 homo- and heterodimers. On the other hand, an increase in mobility was also detected with the GFP-JPH1ΔTMD mutant even if it contains the "joining region." This suggests that removal of either the dimerization domain in the TMD or that in the "joining region" of JPH1 correlates with a decreased association of the resulting mutants with resident JPHs at triads. Interestingly, the ability of JPHs to interact with each other can also explain our previous results, indicating that JPHs have an intrinsic propensity to form clusters with a reduced mobility, even when expressed in nonmuscle cells (46).

In summary, the data reported here indicate that JPH1 and JPH2 can form homo- and heterodimers via interactions established at the level of the TMD and of the cytosolic region. In mature skeletal muscle fibers, the establishing of such interactions with resident JPHs may support the recruitment and retention of newly synthesized JPHs at triads, as observed following expression of full-length and deletion mutants of JPH1 in adult FDB fibers, where triads containing resident JPHs are actually present.

Furthermore, we hypothesize that a similar mechanism of recruitment of JPHs may start operating already in the early stages of embryo development (3, 9, 10, 14, 46). Indeed, the assembly of JPHs in clusters randomly distributed in early embryonal muscle fibers appears to predetermine the membrane domains where peripheral couplings and dyads will form and where proteins of the e-c coupling will be recruited (25–29, 43, 47–52). With the further development of muscle fibers, peripheral couplings and dyads will then evolve to form the triads in adult muscle fibers (3, 9, 10, 13). Accordingly, taking into account the results presented here and the data reported in the literature, we propose a unifying model where JPHs may represent the nucleating system that, by establishing protein-protein interactions, sustains the assembly and the maintenance of junctional membrane domains and the recruitment of e-c coupling proteins, including JPHs, at these sites in both developing and adult skeletal muscle fibers (3, 9–15, 25–29, 46–50). This model may also accommodate recent results that show the requirement of JPH2 in the assembly of MCSs and clustering of key proteins of the e-c coupling process in nonmuscle cells (43).

Materials and Methods

Generation of Expression Vectors. Human Junctophilin-1 (JPH1) (NM_020647) was cloned into the pEGFP-C2 vector (Clontech) using the *Eco*RI sites. Rabbit

Junctophilin-2 (JPH2) (NM_001081998.1) was cloned into the pEGFP-C2 vector (Clontech) using the *Eco*RI sites. Myc-JPH1 and myc-JPH2 were generated by PCR. *Mus musculus* Junctophilin-3 (JPH3) and -4 (JPH4) expression vectors were a gift from Hiroshi Takeshima, Kyoto University, Kyoto, Japan. Plasmids expressing GFP-Extended Synaptotagmin-3, mCherry-Extended Synaptotagmin-3, the PI(4,5)P2 probes iRFP-PH-PLC δ1, GFP-PH-PLC δ1 and the M1 muscarinic acetylcholine receptor (M1R) expression vector have been previously described (42). Sec61β, JPH1, JPH2, JPH3, or JPH4 mutants were generated by PCR using specific primers to amplify the regions of interest. The amplified sequences were cloned in pEGFP-C1, -C2, or -C3 vectors (Clontech), according to the translation reading frame and sequenced using an ABI Prism 7900 apparatus (Applied Biosystem). For experiments using the VSP, the eGFP sequence was replaced by sequences coding for a mRFP-fluorescent protein to obtain plasmid mRFP-JPH1ΔTMD.

For GST pull-down experiments, a region covering the amino acid sequence between MORN VI and MORN VII of *M. musculus* JPH1 (NP_065629.1, amino acids 154 to 278) or JPH2 (NP_001192005.1, amino acids 154–282) was amplified by RT-PCR starting from total RNA from skeletal muscle tissue using sequence-specific primers. cDNAs were cloned into the pGEX4T1 vector (GE Healthcare).

For BiFC, sequences containing the transmembrane domain of JPH1 (NM_020647 amino acids 636 to 661) or the transmembrane domain of JPH4 (NP_796023.2, amino acids 153 to 279) were cloned into pBiFC-VC155 or pBiFC-VN173 vectors. pBiFC-VC155 and pBiFC-VN173 were a gift from Chang-Deng Hu, Department of Medical Chemistry and Molecular Pharmacology, Purdue University, West Lafayette, IN (Addgene plasmids 22010 and 22011).

Cell Cultures and DNA Transfection. Myoblasts were obtained from hind limb muscles of 2-d-old rats (Sprague-Dawley; Harlan). The cell suspension was plated on 0.025% laminin-coated LabTek chambers (Nalge Nunc International) or 0.025% laminin-coated glass coverslips. Cells were grown at 37 °C and 5% CO_2. After 2 d, cells were transfected with the Lipofectamine-Plus method (Invitrogen) following the manufacturer's instructions. Myoblasts were induced to differentiate with α-MEM containing 2 mM L-glutamine (Lonza), 100 μg/mL streptomycin (Lonza), 100 U/mL penicillin (Lonza), 1 mM sodium pyruvate (Lonza), 1 mM dexamethasone (Sigma-Aldrich), 0.05 mM hydrocortisone, supplemented with 10% heat-inactivated FBS (Sigma Aldrich), and 5% heat-inactivated horse serum (Sigma-Aldrich) (49). HeLa cells and HEK293T were cultured in DMEM supplemented with 10% heat-inactivated FBS (Sigma-Aldrich), 2 mM L-glutamine (Sigma-Aldrich), 100 μg/mL streptomycin (Sigma-Aldrich), 100 U/mL penicillin (Lonza), and 1 mM sodium pyruvate (Lonza). Cells were grown at 37 °C and 5% CO_2. Cells were transfected with the Lipofectamine-Plus method (Invitrogen) or with the electroporation system using the Amaxa Nucleofector method (Lonza) and plated on uncoated MatTeks. Imaging was performed 16 to 18 h after the transfection.

Animal Care. Animals were housed in a standard environment maintained at a constant temperature and humidity, and with free access to food and water, following the European legislation on the use and care of laboratory animals (EEC Council Directive 86/609). The animal research was done under the approval of the local ethical committee and the "Ministero della Salute." Animals used for the experiments were either male or female 3-mo-old CD1 mice.

FDB Mouse Skeletal Muscle Fiber Electroporation. Mice were anesthetized with 1.25% 2,2,2-tribromoethanol (Avertin solution; Roche Applied Science) and the FDB muscle was injected with 10 μg of DNA. Two electrodes were placed at each side of the muscle and electric pulses were delivered. Twenty 120-V electric pulses with fixed duration of 20 ms and intervals of 1 s were delivered using an electric pulse generator (Electro Square Poraton ECM830; BTX-Genetronics). Mice were killed 8 d after electroporation (53).

Immunofluorescence Labeling of Differentiated Myotubes and FDB Muscle Fibers. Primary rat myotubes were fixed for 7 min with 3% paraformaldehyde (PFA), 2% sucrose diluted in phosphate buffer saline (PBS) (137 mM NaCl, 2.7 mM KCl, 4.3 mM Na_2HPO_4, 1.4 mM KH_2PO_4) and permeabilized for 3 min in Hepes Triton buffer (20 mM Hepes pH 7.4, 300 mM sucrose, 50 mM NaCl, 3 mM $MgCl_2$, 0.5% Triton X-100). Cells were blocked for 2 h at room temperature in PBS containing 2% bovine serum albumine (BSA, Sigma-Aldrich) and 5% goat serum (Sigma-Aldrich). Nuclei were labeled with 0.1 μg/mL 4′,6-diamidino-2-phenylindole (DAPI) (Sigma-Aldrich) for 10 min at room temperature (54).

Mechanically isolated fibers from electroporated FDB mice were fixed in 1% PFA/0.5% Triton X-100 solution for 1 h at room temperature. The bundles of fibers were further permeabilized with Hepes Triton buffer for 3 min and blocked in 5% goat serum and 2% BSA in PBS for 1 h. To identify the Z-disks, a monoclonal antibody against α-actinin (clone EA-53, Sigma-Aldrich) was used. Triads were labeled with rabbit polyclonal antibodies recognizing RyR (49), mouse monoclonal antibodies against RyR (clone 34C, Thermo Scientific), rabbit polyclonal antibodies against the skeletal muscle isoform of triadin (TRISK95), kindly provided by I. Marty, Université Grenoble Alpes, Grenoble, France, mouse monoclonal antibodies against the dihydropyridine receptor alpha-1 subunit (Thermo Scientific). Cy3 conjugated anti-mouse or anti-rabbit secondary antibodies (Jackson Laboratories) or Alexa Fluor 488 anti-mouse or anti-rabbit secondary antibodies (Thermo Scientific) were used for immunofluorescence detection. In all immunostaining experiments, primary antibodies were prepared in 2% BSA and incubated overnight at 4 °C. Slides were mounted with Mowiol (Mowiol 4-88, Sigma-Aldrich, 20% diluted in PBS) and analyzed with a LSM-510 META confocal microscope (ZEISS, Jena, Germany) as previously described (55). Fibers expressing low levels of GFP fluorescence were selected to avoid potential problems due to overexpression.

Fluorescence Recovery after Photobleaching (FRAP). FRAP experiments were performed on 12-d differentiated rat myotubes, using a confocal laser scanning microscope (ZEISS LSM 510 META). Cells were imaged in buffered medium, containing 140 mM NaCl, 5 mM KCl, 10 mM glucose, 1 mM $MgCl_2$, 0.1 mM $CaCl_2$, 20 mM Hepes, and 0.4 mM EGTA at 37 °C. A 63× 1.4 NA Plan-Apochromat oil immersion objective was used and cells were imaged with a pinhole aperture of 4.96 Airy units, corresponding to a confocal section thickness of 3.5 μm. GFP fluorescence before bleaching and its recovery after bleaching was measured with the 488-nm line of Argon laser with low laser power (0.5%). After the acquisition of 10 prebleached images, a 50% photobleaching was performed using the Argon laser lines 458, 477, and 488 nm. The photobleached area consisted of a circle of 1.08 μm in diameter. Recovery was measured by time lapse imaging at 50- to 300-ms intervals over a period of 1 to 10 min, until fluorescence level reached a plateau. Throughout the experiment fluorescence intensities were acquired for the bleached region (I_{frap}), for the whole cell (I_{whole}) and for the background (I_{base}). Data analyses were performed using the IgorPro software (WaveMetrix, Inc.) (46).

Live Imaging in PI(4,5)P_2 Depletion Experiments. For live imaging in PI(4,5)P_2 depletion in HeLa cells and FDB muscle fibers, see *SI Appendix, SI Materials and Methods*.

Microsome Preparation, Solubilization, and GST Pull Down. Microsomes were prepared from skeletal muscle of CD1 mice or from HEK293T cells. Tissue samples were homogenized in ice-cold buffer A (0.32 M sucrose, 5 mM Hepes pH 7.4, and 0.1 mM phenylmethylsulfonyl fluoride, PMSF) using a potter for cells or a homogenizer for tissues (56). Homogenates were centrifuged at 7,000 × *g* for 5 min at 4 °C. The supernatant was centrifuged at 100,000 × *g* for 1 h at 4 °C. The microsomes were resuspended in buffer A and stored at −80 °C. Protein concentration of the microsomal fraction was quantified using the Bradford protein assay kit (Bio-Rad Laboratories, Hercules, CA). Microsomes prepared from mouse skeletal tissue or from HEK293T cells were solubilized according to the method previously described (49, 56) with some minor modifications. Briefly, microsomes were solubilized at a protein concentration of 1 mg/mL in buffer containing 2% Triton X-100, 1 M NaCl, 1 mM DTT, 20 mM Tris-Cl pH 7.4, and protease inhibitor mixture for 1 h at 4 °C. Microsomes prepared from HEK293T cells were solubilized at a protein concentration of 1 mg/mL for 3 h at 4 °C in buffer containing 10 mM Tris·HCl pH 7.4, 150 mM NaCl, 5 mM EDTA, 1% Triton X-100, 10% glycerol, 1 mM Na_3VO_4, 1 mM PMSF, and protein inhibitor mixture. Solubilized proteins were obtained by centrifugation (Beckman Ti90 rotor) at 48,300 rpm for 45 min at 4 °C. GST pull down was performed as described (57) with some minor modifications. A total of 500 μg of solubilized microsomal proteins were incubated with 25 μg of GST fusion proteins in a buffer containing 10 mM Tris·HCl pH 7.4, 150 mM NaCl, 5 mM EDTA, 1% Triton X-100, 10% glycerol, 1 mM Na_3VO_4, 1 mM PMSF, and protein inhibitor mixture for 2 h at 4 °C. After incubation, the GST fusion protein complexes were washed 3 times with 20 mM Tris-Cl pH 7.4, 150 mM NaCl, and 0.2% Triton X-100. Bound proteins were eluted by boiling in SDS/PAGE sample buffer and subjected to SDS/PAGE (58). Filters were incubated with primary antibodies (for GST pull-down experiments: rabbit anti-JPH1, Thermo Scientific; rabbit anti-JPH2, Thermo Scientific), diluted in blocking buffer overnight at 4 °C with agitation. Filters were washed 3 times with washing buffer (0.5% nonfat dry milk, 50 mM Tris·HCl pH 7.4, 150 mM NaCl, 0.2% Tween-20) for 10 min each, incubated with horseradish peroxidase-conjugated secondary antibody, and detected using the ECL system (ECL Western Blot

Detection Reagents, GE Healthcare) and the Molecular Imager ChemiDoc XRS system (Bio-Rad).

Production and Purification of GST Fusion Proteins. GST fusion proteins were induced in BL21 cells with 1 mM isopropyl β-D-thiogalactopyranoside (IPTG) for 3 h at 30 °C. Cells were harvested and centrifuged at 4,000 rpm for 10 min at 4 °C. The pellet was resuspended in cold buffer containing PBS, 1% Triton X-100, 20 mM EDTA, and lysed by sonication on ice. The soluble fraction was obtained by centrifugation at 13,200 rpm for 15 min at 4 °C. The fusion proteins were immobilized by incubating 1 mL of the soluble fraction with 100 μL of beads of glutathione-Sepharose 4B (GE Healthcare, Buckinghamshire, United Kingdom) for 10 min and washed 3 times with 1 mL of a buffer containing PBS and 1% Triton X-100. Beads were finally resuspended with an equal volume of PBS (49).

Immunoprecipitation and Western Blot Analysis. Immunoprecipitations were performed using the Myc-Trap_A kit (Chromotek) following manufacturer's instructions. Briefly, HEK293T cells were cotransfected with plasmids encoding GFP-JPH1 and myc-JPH1, GFP-JPH2 and myc-JPH1, or GFP-JPH2 and myc-JPH2. Cells were lysed in 10 mM Tris·HCl, pH 7.5, 150 mM NaCl, 0.5 mM EDTA, and 0.5% Nonidet P-40 for 30 min on ice. Cell lysates were added to Myc-Trap_A beads for 1 h at 4 °C. Beads were washed twice with 10 mM Tris·HCl pH 7.5, 500 mM NaCl, and 0.5 mM EDTA. Beads were resuspended in 2× SDS sample buffer (120 mM Tris·HCl pH 6.8, 20% glycerol, 4% SDS, 0.04% bromophenol blue, 10% beta-mercaptoethanol), boiled for 10 min, and analyzed by Western blot using mouse monoclonal anti-myc (Sigma-Merck) or anti-GFP (Thermo Scientific) antibodies. Membranes were first probed with monoclonal anti-GFP antibodies. Following membrane stripping with an appropriate buffer (2% SDS, 100 mM β-mercaptoethanol, 62.5 mM Tris·HCl, pH 6.8; 30 min at 65 °C), membranes were probed with monoclonal anti-myc antibodies.

ACKNOWLEDGMENTS. We thank Yasushi Okamura (University of Osaka) for providing the Ci-VSP plasmid and Hiroshi Takeshima (University of Kyoto) for providing plasmids encoding the cDNA of JPH2, JPH3, and JPH4. This study was supported by grants from Ministry of Health (Grant RF-2013-02356787) and Ministry of Research (MIUR) PRIN 2015 (Grant 2015ZZR4W3) to V.S., and, in part, by NIH Grant NS36251 to P.D.C., and by grants from CNRS, INSERM, and Université Claude Bernard-Lyon 1 to Institut NeuroMyoGène, and by Association Française contre les Myopathies (AFM-Téléthon: Alliance MyoNeurALP program; project 5.3.4.4, to V.J.).

1. Y. Saheki, P. De Camilli, Endoplasmic reticulum-plasma membrane contact sites. *Annu. Rev. Biochem.* **86**, 659–684 (2017).
2. C.-J. Stefan, Building ER-PM contacts: Keeping calm and ready on alarm. *Curr. Opin. Cell Biol.* **53**, 1–8 (2018).
3. C. Franzini-Armstrong, The relationship between form and function throughout the history of excitation-contraction coupling. *J. Gen. Physiol.* **150**, 189–210 (2018).
4. P. Bagnato, V. Barone, E. Giacomello, D. Rossi, V. Sorrentino, Binding of an ankyrin-1 isoform to obscurin suggests a molecular link between the sarcoplasmic reticulum and myofibrils in striated muscles. *J. Cell Biol.* **160**, 245–253 (2003).
5. E. Giacomello *et al*., Deletion of small ankyrin 1 (sAnk1) isoforms results in structural and functional alterations in aging skeletal muscle fibers. *Am. J. Physiol. Cell Physiol.* **308**, C123–C138 (2015).
6. D. Randazzo *et al*., Exercise-induced alterations and loss of sarcomeric M-line organization in the diaphragm muscle of obscurin knockout mice. *Am. J. Physiol. Cell Physiol.* **312**, C16–C28 (2017).
7. D. Randazzo, E. Pierantozzi, D. Rossi, V. Sorrentino, The potential of obscurin as a therapeutic target in muscle disorders. *Expert Opin. Ther. Targets* **21**, 897–910 (2017).
8. C. Franzini-Armstrong, Studies of the triad: I. Structure of the junction in frog twitch muscles. *J. Cell Biol.* **47**, 488–499 (1970).
9. H. Takekura, B.-E. Flucher, C. Franzini-Armstrong, Sequential docking, molecular differentiation, and positioning of T-Tubule/SR junctions in developing mouse skeletal muscle. *Dev. Biol.* **239**, 204–214 (2001).
10. B.-E. Flucher, S.-B. Andrews, M.-P. Daniels, Molecular organization of transverse tubule/sarcoplasmic reticulum junctions during development of excitation-contraction coupling in skeletal muscle. *Mol. Biol. Cell* **5**, 1105–1118 (1994).
11. E. Ríos, G. Pizarro, E. Stefani, Charge movement and the nature of signal transduction in skeletal muscle excitation-contraction coupling. *Annu. Rev. Physiol.* **54**, 109–133 (1992).
12. R.-T. Rebbeck *et al*., Skeletal muscle excitation-contraction coupling: Who are the dancing partners? *Int. J. Biochem. Cell Biol.* **48**, 28–38 (2014).
13. E. Ríos, Calcium-induced release of calcium in muscle: 50 years of work and the emerging consensus. *J. Gen. Physiol.* **150**, 521–537 (2018).
14. H. Takeshima, S. Komazaki, M. Nishi, M. Iino, K. Kangawa, Junctophilins: A novel family of junctional membrane complex proteins. *Mol. Cell* **6**, 11–22 (2000).
15. K. Ito *et al*., Deficiency of triad junction and contraction in mutant skeletal muscle lacking junctophilin type 1. *J. Cell Biol.* **154**, 1059–1067 (2001).
16. M. Nishi, H. Sakagami, S. Komazaki, H. Kondo, H. Takeshima, Coexpression of junctophilin type 3 and type 4 in brain. *Brain Res. Mol. Brain Res.* **118**, 102–110 (2003).
17. H. Takeshima, M. Hoshijima, L. S. Song, Ca^{2+} microdomains organized by junctophilins. *Cell Calcium* **58**, 349–356 (2015).
18. S. Kakizawa, S. Moriguchi, A. Ikeda, M. Iino, H. Takeshima, Functional crosstalk between cell-surface and intracellular channels mediated by junctophilins essential for neuronal functions. *Cerebellum* **7**, 385–391 (2008).
19. M. Kirmiz *et al*., Remodeling neuronal ER-PM junctions is a conserved nonconducting function of Kv2 plasma membrane ion channels. *Mol. Biol. Cell* **29**, 2410–2432 (2018).
20. S. Moriguchi *et al*., Functional uncoupling between Ca^{2+} release and after-hyperpolarization in mutant hippocampal neurons lacking junctophilins. *Proc. Natl. Acad. Sci. U.S.A.* **103**, 10811–10816 (2006).
21. L. Li *et al*., Junctophilin 3 expresses in pancreatic beta cells and is required for glucose-stimulated insulin secretion. *Cell Death Dis.* **7**, e2275 (2016).
22. J.-S. Woo *et al*., Junctophilin-4, a component of the endoplasmic reticulum-plasma membrane junctions, regulates Ca^{2+} dynamics in T cells. *Proc. Natl. Acad. Sci. U.S.A.* **113**, 2762–2767 (2016).
23. A. Garbino *et al*., Molecular evolution of the junctophilin gene family. *Physiol. Genomics* **37**, 175–186 (2009).
24. H.-J. Bennett *et al*., Human junctophilin-2 undergoes a structural rearrangement upon binding PtdIns(3,4,5)P_3 and the S101R mutation identified in hypertrophic cardiomyopathy obviates this response. *Biochem. J.* **456**, 205–217 (2013).
25. A.-J. Phimister *et al*., Conformation-dependent stability of junctophilin 1 (JP1) and ryanodine receptor type 1 (RyR1) channel complex is mediated by their hyper-reactive thiols. *J. Biol. Chem.* **282**, 8667–8677 (2007).
26. R.-J. van Oort *et al*., Disrupted junctional membrane complexes and hyperactive ryanodine receptors after acute junctophilin knockdown in mice. *Circulation* **123**, 979–988 (2011).
27. L. Golini *et al*., Junctophilin 1 and 2 proteins interact with the L-type Ca2+ channel dihydropyridine receptors (DHPRs) in skeletal muscle. *J. Biol. Chem.* **286**, 43717–43725 (2011).
28. T. Nakada *et al*., Physical interaction of junctophilin and the $Ca_V1.1$ C terminus is crucial for skeletal muscle contraction. *Proc. Natl. Acad. Sci. U.S.A.* **115**, 4507–4512 (2018).
29. J.-S. Woo *et al*., Glutamate at position 227 of junctophilin-2 is involved in binding to TRPC3. *Mol. Cell. Biochem.* **328**, 25–32 (2009).
30. S. Minamisawa *et al*., Junctophilin type 2 is associated with caveolin-3 and is down-regulated in the hypertrophic and dilated cardiomyopathies. *Biochem. Biophys. Res. Commun.* **325**, 852–856 (2004).
31. A.-P. Landstrom *et al*., Mutations in JPH2-encoded junctophilin-2 associated with hypertrophic cardiomyopathy in humans. *J. Mol. Cell. Cardiol.* **42**, 1026–1035 (2007).
32. A.-P. Landstrom *et al*., Junctophilin-2 expression silencing causes cardiocyte hypertrophy and abnormal intracellular calcium-handling. *Circ. Heart Fail.* **4**, 214–223 (2011).
33. Y. Matsushita *et al*., Mutation of junctophilin type 2 associated with hypertrophic cardiomyopathy. *J. Hum. Genet.* **52**, 543–548 (2007).
34. A.-P. Quick *et al*., Novel junctophilin-2 mutation A405S is associated with basal septal hypertrophy and diastolic dysfunction. *JACC Basic Transl. Sci.* **2**, 56–67 (2017).
35. S. U. M. Vanninen *et al*., Heterozygous junctophilin-2 (JPH2) p.(Thr161Lys) is a monogenic cause for HCM with heart failure. *PLoS One* **13**, e0203422 (2018).
36. C. Pinali *et al*., Post-myocardial infarction T-tubules form enlarged branched structures with dysregulation of junctophilin-2 and bridging integrator 1 (BIN-1). *J. Am. Heart Assoc.* **6**, e004834 (2017).
37. O. Manfra, M. Frisk, W.-E. Louch, Regulation of cardiomyocyte T-tubular structure: Opportunities for therapy. *Curr. Heart Fail. Rep.* **14**, 167–178 (2017).
38. H. B. Zhang *et al*., Ultrastructural uncoupling between T-tubules and sarcoplasmic reticulum in human heart failure. *Cardiovasc. Res.* **98**, 269–276 (2013).
39. C. Zhang *et al*., Microtubule-mediated defects in junctophilin-2 trafficking contribute to myocyte transverse-tubule remodeling and Ca2+ handling dysfunction in heart failure. *Circulation* **129**, 1742–1750 (2014).
40. C. Y. Wu *et al*., Calpain-dependent cleavage of junctophilin-2 and T-tubule remodeling in a mouse model of reversible heart failure. *J. Am. Heart Assoc.* **3**, e000527 (2014).
41. G. Di Paolo, P. De Camilli, Phosphoinositides in cell regulation and membrane dynamics. *Nature* **443**, 651–657 (2006).
42. F. Giordano *et al*., PI(4,5)P(2)-dependent and $Ca^{(2+)}$-regulated ER-PM interactions mediated by the extended synaptotagmins. *Cell* **153**, 1494–1509 (2013).
43. S. Perni, M. Lavorato, K. G. Beam, De novo reconstitution reveals the proteins required for skeletal muscle voltage-induced Ca^{2+} release. *Proc. Natl. Acad. Sci. U.S.A.* **114**, 13822–13827 (2017).
44. Y. Murata, H. Iwasaki, M. Sasaki, K. Inaba, Y. Okamura, Phosphoinositide phosphatase activity coupled to an intrinsic voltage sensor. *Nature* **435**, 1239–1243 (2005).
45. C. Berthier, C. Kutchukian, C. Bouvard, Y. Okamura, V. Jacquemond, Depression of voltage-activated Ca^{2+} release in skeletal muscle by activation of a voltage-sensing phosphatase. *J. Gen. Physiol.* **145**, 315–330 (2015).
46. V. Cusimano, F. Pampinella, E. Giacomello, V. Sorrentino, Assembly and dynamics of proteins of the longitudinal and junctional sarcoplasmic reticulum in skeletal muscle cells. *Proc. Natl. Acad. Sci. U.S.A.* **106**, 4695–4700 (2009).

47. V. Barone, D. Randazzo, V. Del Re, V. Sorrentino, D. Rossi, Organization of junctional sarcoplasmic reticulum proteins in skeletal muscle fibers. *J. Muscle Res. Cell Motil.* **36**, 501–515 (2015).
48. L. Al-Qusairi, J. Laporte, T-tubule biogenesis and triad formation in skeletal muscle and implication in human diseases. *Skelet. Muscle* **1**, 26 (2011).
49. D. Rossi *et al*., Distinct regions of triadin are required for targeting and retention at the junctional domain of the sarcoplasmic reticulum. *Biochem. J.* **458**, 407–417 (2014).
50. C.-C. Yin, F.-A. Lai, Intrinsic lattice formation by the ryanodine receptor calcium-release channel. *Nat. Cell Biol.* **2**, 669–671 (2000).
51. A. Osseni *et al*., Triadin and CLIMP-63 form a link between triads and microtubules in muscle cells. *J. Cell Sci.* **129**, 3744–3755 (2016).
52. S. A. Goonasekera *et al*., Triadin binding to the C-terminal luminal loop of the ryanodine receptor is important for skeletal muscle excitation contraction coupling. *J. Gen. Physiol.* **130**, 365–378 (2007).
53. V. Barone *et al*., Yip1B isoform is localized at ER-Golgi intermediate and cis-Golgi compartments and is not required for maintenance of the Golgi structure in skeletal muscle. *Histochem. Cell Biol.* **143**, 235–243 (2015).
54. E. Pierantozzi *et al*., Tissue-specific cultured human pericytes: Perivascular cells from smooth muscle tissue have restricted mesodermal differentiation ability. *Stem Cells Dev.* **25**, 674–686 (2016).
55. V. Barone *et al*., Identification and characterization of three novel mutations in the CASQ1 gene in four patients with tubular aggregate myopathy. *Hum. Mutat.* **38**, 1761–1773 (2017).
56. X. Altafaj *et al*., Maurocalcine interacts with the cardiac ryanodine receptor without inducing channel modification. *Biochem. J.* **406**, 309–315 (2007).
57. D. Rossi *et al*., A novel FLNC frameshift and an OBSCN variant in a family with distal muscular dystrophy. *PLoS One* **12**, e0186642 (2017).
58. D. Rossi *et al*., Expression and functional activity of ryanodine receptors (RyRs) during skeletal muscle development. *Cell Calcium* **41**, 573–580 (2007).